

# Effective pinhole-collimated ultrasmall-angle x-ray scattering instrument for measuring anisotropic microstructures

J. Ilavsky<sup>a)</sup>

*University of Maryland, College Park, Maryland 20742*

A. J. Allen and G. G. Long

*National Institute of Standards and Technology, Gaithersburg, Maryland 20899*

P. R. Jemian

*University of Illinois, Urbana-Champaign, Illinois 61801*

(Presented on 22 August 2001)

Small-angle scattering is widely used for measuring materials microstructure in the 1–100 nm size range. Ultrasmall-angle x-ray scattering (USAXS), typically achieved through crystal collimation, extends this size range to include features over 1  $\mu\text{m}$  in size. This article reports on USAXS on the UNICAT beam line 33-ID at the Advanced Photon Source. The instrument makes use of a six-reflection crystal pair as a collimator and another six-reflection crystal pair as an analyzer. First principle absolute calibration and a broad scattering vector range make this a very effective instrument, limited only by the fact that the measurement of anisotropic microstructures is excluded due to slit smearing from the crystal collimation. This limitation has recently been removed by adding a horizontally reflecting crystal before and another after the sample. This creates a USAXS instrument with collimation in two orthogonal directions. We call this configuration effective pinhole USAXS. Now, anisotropic materials are probed using 9–17 keV photons in the same physically-relevant (from 50 nm to over 1  $\mu\text{m}$ ) microstructural size range as that available for materials which scatter isotropically. © 2002 American Institute of Physics.

[DOI: 10.1063/1.1425387]

## I. INTRODUCTION

Ultrasmall-angle x-ray scattering (USAXS) utilizes Bonse–Hart double-crystal optics<sup>1</sup> to extend the range of SAXS down to lower scattering vectors,  $\mathbf{Q}$ , where  $|\mathbf{Q}| = (4\pi/\lambda)(\sin \theta)$  and  $2\theta$  is the scattering angle. However, when the instrument is used in its standard configuration, the measured USAXS data are smeared by the collimation of the vertically diffracting crystals. With the addition of a pair of horizontally reflecting crystals, slit smearing is removed, and an effective-pinhole collimation is achieved. This is at a small cost in intensity dynamic range and reduced  $Q$  range. However, effective-pinhole USAXS enables the characterization of anisotropic microstructures with nearly the same high resolution that had previously only been available for measurements of isotropic materials.

As an example of the capabilities of the new instrument, we will show scattering results from ceramic coatings. Thermally sprayed (TS) and electron-beam (EB) physical vapor-deposited yttria-stabilized zirconia (YSZ) coatings (8 mass % by volume  $\text{Y}_2\text{O}_3$  in  $\text{ZrO}_2$ ) are routinely used by industry as thermal barrier deposits in engines and turbines. These deposits have become increasingly important with the impetus for higher efficiency and cleaner burning of fuel.

The porous phase within these deposits is one of the features of their microstructure that controls their properties and performance. Both TS and EB processes can produce a

wide range of microstructures, with varying engineering properties. Major problems are still encountered by industrial users and researchers seeking to characterize the void microstructure quantitatively. One of the problems is that both microstructures include multiple void systems, some of which (e.g., interlamellar pores and intralamellar cracks for TS or vertical intercolumnar voids for EB) are anisotropic and some (e.g., globular porosity for TS) are isotropic. Since the voids generally exhibit irregular shapes and a large range of sizes, as well as both open and closed porosity, their characterization by standard volumetric techniques (intrusion techniques) is insufficient. Since the material is also fragile, reliable preparation of electron microscopy samples is difficult. Hence, there is a need for advanced techniques such as effective pinhole USAXS or grazing incidence small-angle scattering.

## II. INSTRUMENT AND DATA ACQUISITION

The UNICAT ultrasmall-angle x-ray scattering instrument<sup>2</sup> has used to measure data with very high  $\mathbf{Q}$  resolution ( $\sim 1.5 \times 10^{-4} \text{ \AA}^{-1}$ ) in the vertical direction but is slit smeared in the horizontal direction (slit length  $\sim 0.05 \text{ \AA}^{-1}$  depending on geometry). For isotropic microstructures, the measured scattering data can be numerically desmeared to recover the standard (pinhole-collimated) small-angle scattering data. For anisotropic microstructures, however, such information cannot be recovered. This limitation to isotropic microstructures has been removed by adding two

<sup>a)</sup>Electronic mail: ilavsky@aps.anl.gov

### Effective Pinhole-Collimated USAXS

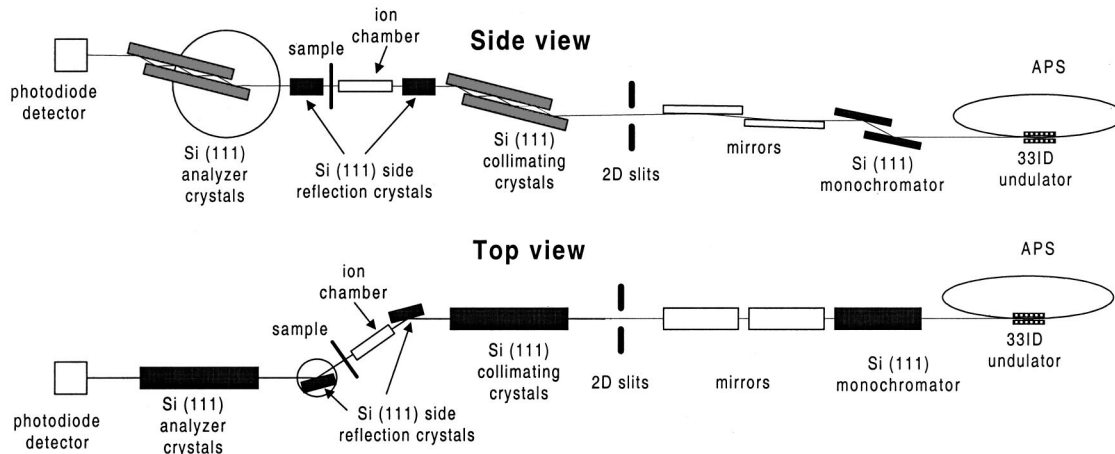


FIG. 1. Schematic of the effective pinhole-collimated USAXS instrument at UNICAT.

horizontally diffracting crystals,<sup>3</sup> which collimate the measured USAXS in two orthogonal directions providing, in effect, pinhole collimation (see Fig. 1) with  $Q$  resolution about  $1.5 \times 10^{-4} \text{ \AA}^{-1}$  in both directions. With this collimation, the need for numerical desmearing of the data is removed.

The basic advantages of the UNICAT USAXS instrument are that it offers a first-principles absolute calibration of

the data (no need for a secondary standard), a broad intensity range (up to nine orders of magnitude), and a broad  $|Q|$  range ( $1.2 \times 10^{-4} \text{ \AA}^{-1} < |Q| < 0.1 \text{ \AA}^{-1}$  [ $1 \text{ \AA}^{-1}$  for slit smeared configuration]). Examples of effective pinhole blank scans (with no sample in place) are shown in Fig. 2.

The incident beam is defined by the incoming slits to less than  $0.4 \text{ mm} \times 0.4 \text{ mm}$ . Samples are centered on the rotational axis of an azimuthal rotational stage, which is centered on the x-ray beam. For each  $|Q|$ , the horizontally reflecting crystal after the sample is rotated to maintain the Bragg condition, and the analyzer pair of crystals is set to the appropriate angle. Two-dimensional scattering data are measured as the sample azimuth ( $\alpha$ ), the second horizontally reflecting crystal and the analyzer crystal pair are scanned. The effective-pinhole configuration of this instrument was tested between 9 and 17 keV. At the upper-end of this range, the x-ray absorption is low enough so that even  $200\text{-}\mu\text{m}$ -thick YSZ deposits can be studied.

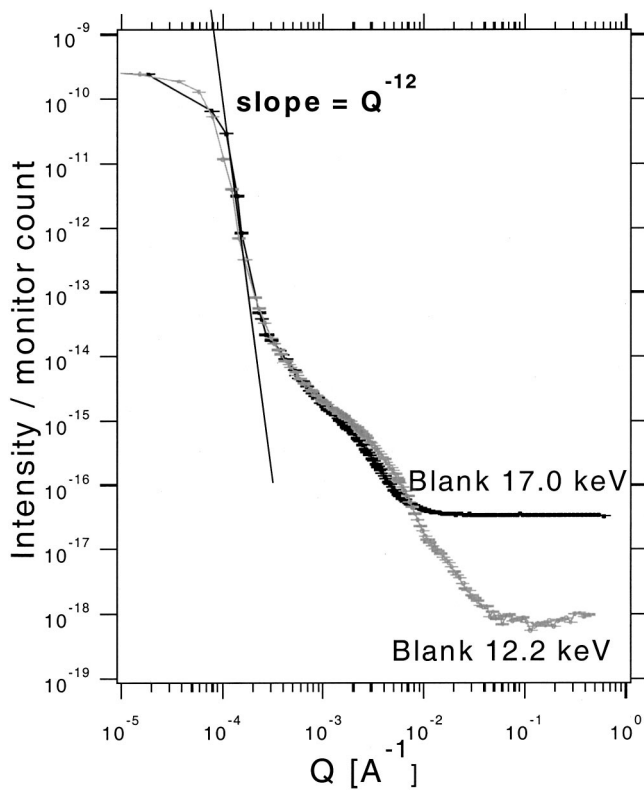


FIG. 2. Instrumental curves (blank) for effective pinhole-collimated USAXS using 17.0 and 12.2 keV incident photons. The intensity range as well as the  $Q$  range are energy and slit size dependent. At 17 keV, with  $0.1 \text{ mm} \times 0.1 \text{ mm}$  slits, the intensity range is only about 7 decades, whereas at 12.2 keV, with  $0.3 \text{ mm} \times 0.3 \text{ mm}$  slits, the intensity range is over 8 decades. Note the power law dependence at low  $Q$  where  $I \sim Q^{-12}$  which is expected for the six reflections in the crystal pair. The errors in intensity and scattering vector are smaller than the sizes of the data points.

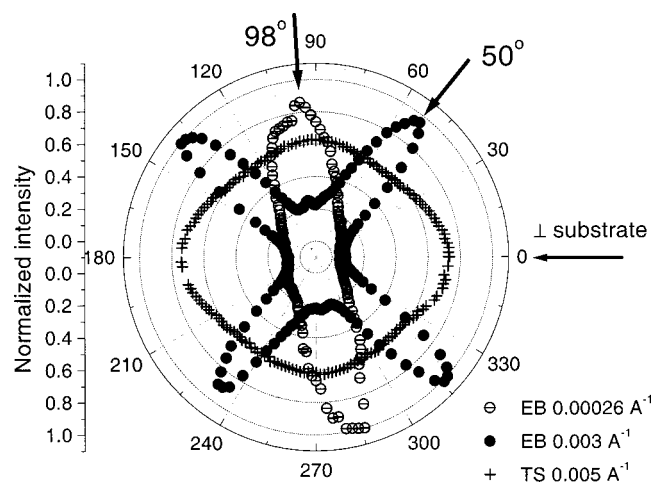


FIG. 3. Scattering intensity as a function of azimuthal angle  $\alpha$  for the EB YSZ at  $Q=0.00026$  and  $0.003 \text{ \AA}^{-1}$ , and for TS YSZ at  $Q=0.005 \text{ \AA}^{-1}$ . Note the strong differences in anisotropy at different  $Q$ , within a single sample. The arrow near 0 indicates the direction perpendicular to the substrate surface. The errors are within the sizes of the data points.

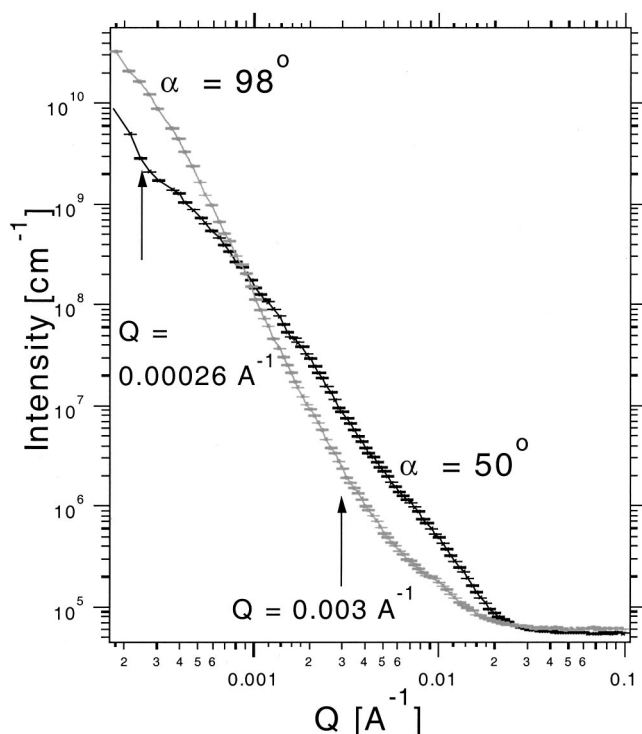


FIG. 4. Log-log plot of USAXS absolute calibrated data from EB sample measured with azimuth angle  $50^\circ$  and  $98^\circ$ . Note the correspondence to data (marked with arrows) in Fig. 3.

Typically, small-angle scattering data are collected in  $5^\circ$  steps in sample azimuth ( $\alpha$ ). Two methods are usually combined. In the first, the scattered intensity is measured as a function of  $Q$  for each orientation  $\alpha$ . Alternatively the scattered intensity at particular  $Q$  can be measured as a function of  $\alpha$ . Such scans provide a quantitative map of the anisotropy of the microstructure as a function of the sizes of the scattering populations. Figure 3 shows examples of data from TS and EB YSZ samples accumulated by the latter method. The differences in anisotropy of the scattering are related to the different sizes and anisotropies of the microstructures. The effective pinhole data shown in Fig. 4 were measured from the EB sample using the former method. Note the arrows in Figs. 3 and 4, which indicate corresponding azimuthal positions  $\alpha$ .

By combining the data from the two methods described above, the full two-dimensional scattering pattern, similar to the pattern from pinhole collimated instruments with area detectors, can be obtained. However, the resulting data enjoy the high  $Q$  resolution and large  $Q$  range of the USAXS geometry.

The data in the Fig. 3 obtained for TS YSZ deposits can be evaluated using the method of anisotropic Porod scattering.<sup>4</sup> The complex shape in this figure can be separated into two orthogonal ellipsoids and, using the rotational symmetry of the microstructure (direction perpendicular to the substrate), the scattering over all  $4\pi$  can be reconstructed. Therefore one can obtain the total surface areas in the two major anisotropic void systems—interlamellar pores and intralamellar cracks.

The results (Fig. 3) obtained from EB YSZ deposits show that at  $Q=0.00026 \text{ \AA}^{-1}$  (large void sizes) the scattering is strong in the direction parallel to the substrate and as the  $Q$  increases to  $0.003 \text{ \AA}^{-1}$  (void sizes decrease) the anisotropy changes into more complex orientation with maxima around  $50^\circ$  from the direction perpendicular to the substrate. The large features within the microstructures are intercolumnar pores, which are preferentially perpendicular to this surface, whereas the small features are intra-columnar growth-related voids, which are very difficult, if not impossible, to characterize by other methods. Their orientation is, as our results indicate for this sample, tilted towards the substrate surface. Note, that these growth-related voids vary significantly with manufacturing method.

### III. CONCLUSIONS

Effective pinhole USAXS provides a practical means to characterize the microstructures of anisotropic materials. Such characterizations can now be carried out on thicker materials and materials more relevant to industry without the added complications of grazing angle geometry.

### ACKNOWLEDGMENTS

The UNICAT facility at the Advanced Photon Source (APS) is supported by the University of Illinois at Urbana-Champaign, Materials Research Laboratory [U.S. Department of Energy (DOE), the State of Illinois-IBHE-HECA, and the National Science Foundation], the Oak Ridge National Laboratory (U.S. DOE), the National Institute of Standards and Technology (U.S. Department of Commerce), and UOP LLC. Use of APS is supported by the U.S. DOE, Basic Energy Sciences, Office of Science, under Contract No. W-31-109-ENG-38.

<sup>1</sup>U. Bonse and M. Hart, *Appl. Phys. Lett.* **7**, 238 (1965).

<sup>2</sup>G. G. Long, A. J. Allen, J. Ilavsky, P. R. Jemian, and P. Zschack, *AIP Conf. Proc.* **521**, 183 (2000).

<sup>3</sup>U. Bonse and M. Hart, *Z. Phys.* **189**, 151 (1966).

<sup>4</sup>J. Ilavsky, G. G. Long, A. J. Allen, and C. C. Berndt, *Mater. Sci. Eng., A* **272**, 215 (1999).